Analysis of hard x-ray focusing by 2D diamond CRL

Chubar, Oleg, Wiegart, Lutz, Antipov, Sergey, Celestre, Rafael, Coles, Rebecca, et al.

Oleg Chubar, Lutz Wiegart, Sergey Antipov, Rafael Celestre, Rebecca Coles, Andrei Fluerasu, Maksim Rakitin, "Analysis of hard x-ray focusing by 2D diamond CRL," Proc. SPIE 11493, Advances in Computational Methods for X-Ray Optics V, 114930M (21 August 2020); doi: 10.1117/12.2568980

SPIE.

Event: SPIE Optical Engineering + Applications, 2020, Online Only

Analysis of hard X-ray focusing by 2D diamond CRL

Oleg Chubar*[a], Lutz Wiegart[a], Sergey Antipov[b], Rafael Celestre[c], Rebecca Coles[a], Andrei Fluerasu[a], Maksim Rakitin[a]

[a]National Synchrotron Light Source II, Brookhaven National Laboratory, NY 11973, USA; [b]Euclid Techlabs LLC, Bolingbrook, IL 60440 USA; [c]European Synchrotron Radiation Facility, 71 Avenue des Martyrs, CS 40220, 38043 Grenoble Cedex 9, France

ABSTRACT

X-ray Compound Refractive Lenses (CRLs) made out of diamond have a number of attractive features for applications at modern light sources, such as relatively large refractive index decrement and yet relatively low absorption for hard X-rays, low thermal expansion coefficient and high mechanical rigidity (allowing to safely use them as first optical elements of beamlines), and relatively low undesirable scattering from their volume. However, diamond CRLs are hard to fabricate and process to a (sub-)micron accuracy of the surface shape, required for aberration-free focusing of hard X-rays. We will report on results of experimental tests of first generation 2D diamond CRLs manufactured by Euclid Techlabs LLC. The tests were performed at the Coherent Hard X-ray beamline of the National Synchrotron Light Source II, and included measurements of intensity profiles of ~13 keV undulator radiation focused by one diamond lens in a low-demagnification geometry. Such geometry is typically used for the X-ray beam transport and can be used for the imaging-based diagnostics of the emitting electron beam. The quality of X-ray focusing with the new diamond CRL was analyzed by comparing the measurement results with partially-coherent wave-optics simulations performed with Synchrotron Radiation Workshop code. The tests of the diamond CRL also included measurements of small-angle X-ray scattering produced by it, and comparison of these data with the scattering data from a beryllium CRL with the same focal length.

Keywords: synchrotron radiation, light sources, diamond CRL, X-ray focusing

1. INTRODUCTION

Compound Refractive Lenses are currently very popular optics for hard X-rays, and their popularity only keeps on increasing since their invention in 1996 [1]. Due to small values of the refractive index decrement for many materials ($\sim 10^{-6}$ - 10^{-5}) in the hard X-ray spectral range, to reach high-quality focusing of a hard X-ray beam, the accuracy of CRL surface shape, that is required to be parabolic in one or two dimensions, has to be on the order of sub-micron. This is a more "relaxed" requirement than e.g. the (sub-) 10 nm surface height error requirement that is applied to grazing-incidence X-ray mirrors. As refractive optical elements, CRLs are used in ~normal incidence, and therefore have much smaller dimensions than X-ray mirrors. Because of these factors, CRLs are usually easier to manufacture to a required accuracy than X-ray mirrors, which results in their lower manufacturing costs. The manufacturing costs of CRLs are also lower than for other types of X-ray optics, such as zone plates [2] or Multi-Layer Laue lenses [3, 4], having fine structure of zones / layers, requiring very high positioning accuracy and often advanced technology for their production.

Among disadvantages of CRLs, one can mention their chromaticity and requirement of using large numbers of individual lenses for strong focusing of hard X-rays down to sub-micron spot sizes. These disadvantages, however, do not pose any problems for using CRLs as transport optics in hard X-ray beamlines, especially those that don't require continuous variation of photon energy. When used in this role, CRLs usually preserve well wavefront quality and coherence properties of X-ray beam [5], which makes their application particularly attractive in high-brightness and high-coherence light sources of most recent generations – ultra-small-emittance multi-bend achromat type storage rings [6, 7] and X-ray free-electron lasers [8, 9].

*chubar@bnl.gov; phone 1 631 344-4525

Advances in Computational Methods for X-Ray Optics V, edited by Oleg Chubar, Kawal Sawhney, Proc. of SPIE Vol. 11493, 114930M · © 2020 SPIE
CCC code: 0277-786X/20/$21 · doi: 10.1117/12.2568980

The choice of materials for producing CRLs is a very special topic. Such material properties as relatively large refractive index decrement and yet relatively low absorption of hard X-rays, low thermal expansion coefficient, high mechanical rigidity, high melting temperature, absence of degradation under extended exposure to X-rays, and possibility to perform high-accuracy processing / surface shaping, are very important for CRLs [10]. The very first CRLs were manufactured out of aluminum, by simple (though still high accuracy) "drilling" of holes in the bulk of material. Shortly after this, more advanced manufacturing techniques, allowing to produce parabolic-shape lenses, started to be used for the production of aluminum and beryllium CRLs [11, 12].

Beryllium parabolic CRL [12] is currently probably the most popular type of CRL, extensively used at hard X-ray beamlines of modern light source facilities. Beryllium has attractive refractive index and very low absorption coefficient for hard X-rays (considerably lower than that of aluminum); it doesn't degrade under long-term exposure to X-rays; it can be processed to the required sub-micron surface shape accuracy level, even though its processing has to be performed with special precautions because of the toxicity of beryllium-containing dust. The thermal and mechanical properties of beryllium are appropriate for applications at light sources with monochromatic X-rays, however, cases are known when Be CRL, used as a first optical element of a beamline, was destroyed after long direct exposure to intense polychromatic "white" beam of undulator radiation [13]. A less attractive property of beryllium is its inhomogeneity over the volume on (sub-)micron level (depending on its grade) that often results in undesirable scattering of X-rays at their propagation through the volume of material [14, 15].

Diamond has even more attractive properties than beryllium as potential material for CRL. Even though its absorption is higher, it is usually "compensated" by larger refractive index decrement, so that larger radius of surface curvature and / or smaller number of individual lenses is required for obtaining a necessary focal length with diamond CRL than with beryllium one. Volume homogeneity, thermal and mechanical properties of diamond are much better than these of beryllium. The only (however, quite substantial) "problem" with diamond is a difficulty of its processing / machining with sub-micron accuracy for obtaining the required quality of the parabolic CRL surface shape. This problem was recently overcome by several companies, who developed necessary technologies for machining and polishing diamond CRLs [16, 17]. The developed technology [17] is based on femtosecond laser microfabrication. Unlike nanosecond pulses from standard laser cutters for diamonds, femtosecond pulses are so short that they only ablate the material and do not lead to thermal fatigue, subsequent crystalline defect formation. As ablated, diamond lens surface roughness is on the order of 300nm, which is almost acceptable for refractive optics [12]. To further reduce the roughness, the lens can be polished using Chemical Mechanical Polishing method [18] down to ~20 nm arithmetical mean height surface roughness, fully satisfying the requirement for X-ray focusing.

In this paper, we describe experimental tests of hard X-ray focusing by a first-generation diamond CRL [17] in a low-demagnification geometry, and measurements of Small Angle X-ray Scattering (SAXS) from this CRL in the same geometry, in comparison with the scattering produced by an equivalent Be CRL. The tests were performed at the Coherent Hard X-ray (CHX) beamline of the National Synchrotron Light Source II (NSLS-II) in the Brookhaven National Laboratory.

2. MESUREMENTS AND CALCULATIONS OF X-RAY FOCUSING

2.1 Experimental layout

The experimental layout used for the measurements of X-ray focusing with 2D diamond CRL at CHX beamline is shown in figure 1. The X-ray source at CHX is a 20 mm period 3 m long in-vacuum undulator (U20) installed in a low-beta straight section of NSLS-II. The Undulator Radiation (UR) from this source passed through flat harmonic rejection mirror (not shown in figure 1) and then through a Si(111) Double-Crystal Monochromator (DCM) that was tuned to ~13.5 keV photon energy (the X-rays at this photon energy were emitted at 7th harmonic of UR spectrum). This radiation was then focused by a 2D diamond CRL located at ~48.7 m from the center of U20. The CRL had ~400 μm diameter of its circular geometrical aperture and consisted of one concave lens formed by two surfaces having shapes of paraboloids of rotation with ~100 μm radius of curvature at the tip of parabola A variable-size rectangular aperture was placed in front of the CRL.

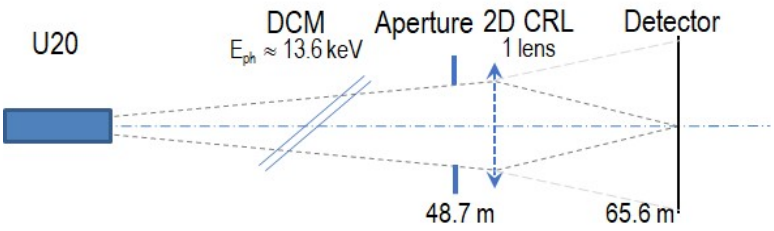

Figure 1. Experimental layout for measurements of intensity distributions of hard X-rays of undulator radiation focused with CRL at the CHX beamline.

The intensity distributions of the focused X-rays were measured by means of an imaging detector and with a fluorescent knife-edge setup. The imaging detector was based on a fluorescent screen, magnification optics and a CCD camera [19]. Limited by optical resolution and linearity of the fluorescence signal, 2D detector images were collected for alignment tests and to visualize the 2D intensity distributions. The fluorescent knife-edge measurements used for the quantitative analysis of the focal spot size were based on the fluorescence signal from a 50 nm thick Cr layer deposited atop a thin and approximately 200 μm tall 'wall' etched into a silicon wafer. Two such knife-edges were mounted in an L-configuration on a nanometer precision hexapod for alignment and scanning, and the fluorescence signal from the Cr layer was collected with an energy dispersive detector [19].

The experimental layout shown in figure 1 was used previously for high-accuracy measurements of the horizontal and vertical electron beam emittances in the NSLS-II storage ring by means of a 2D Be CRL [20]. In this layout, a good-quality Be CRL was creating a de-magnified image of the electron beam profile in the detector plane (located at ~65.6 m from the center of undulator). The horizontal size of the X-ray beam in the detector plane (~32 μm as measured) was dominated by the horizontal size of the electron beam, whereas its vertical size (~5.4 μm as measured) was dominated by the diffraction-limited single-electron focused UR intensity distribution (i.e. the "point-spread function" of the optical system). It was decided to perform tests of the diamond CRL in the same geometry, benefiting from the close (~12.5 m) focal length values of the two CRLs for ~13 keV photon energy X-rays.

2.2 Measurement results of X-ray focusing with 2D diamond CRL

The preliminary test images of intensity distributions of the 13.54 keV X-rays focused with 2D diamond CRL, performed using the imaging detector, are shown in figure 2 (a, b). The image in figure 2 (a) was "taken" with the rectangular aperture located before the CRL open to 400 x 400 μm^2 to fully accommodate the geometrical circular aperture of the CRL, while the image shown in figure 2 (b) corresponds to a smaller, 100 μm (h) x 200 (v) μm, aperture. Unfortunately, these images appeared to be partially saturated and could not be used for numerical analysis. However, they clearly illustrate that at the fully open geometrical aperture of the CRL, the focused spot contains quite considerable aberrations – "side lobes" / secondary intensity maxima, located below and above the main maximum.

For comparison, we also present in figure 2 (c, d) intensity distributions of the focused partially coherent UR calculated using the SRW code [21, 22] under Sirepo web-based interface [23] at the assumption of perfect paraboloid of rotation shape of 2D diamond CRL. At these and other partially-coherent wave propagation calculations presented in this paper, the following lattice and electron beam parameters in the low-beta straight section of the NSLS-II were used: horizontal and vertical beta functions equal to 1.84 m and 1.17 m respectively, horizontal and vertical emittances equal to 0.76 nm and 30 pm, resulting in ~37.5 μm horizontal and ~5.9 μm vertical RMS electron beam sizes in the middle of the straight section. We note that the intensity distributions measured previously with Be CRL were quite close to calculated intensity distributions shown in figure 2 (c, d).

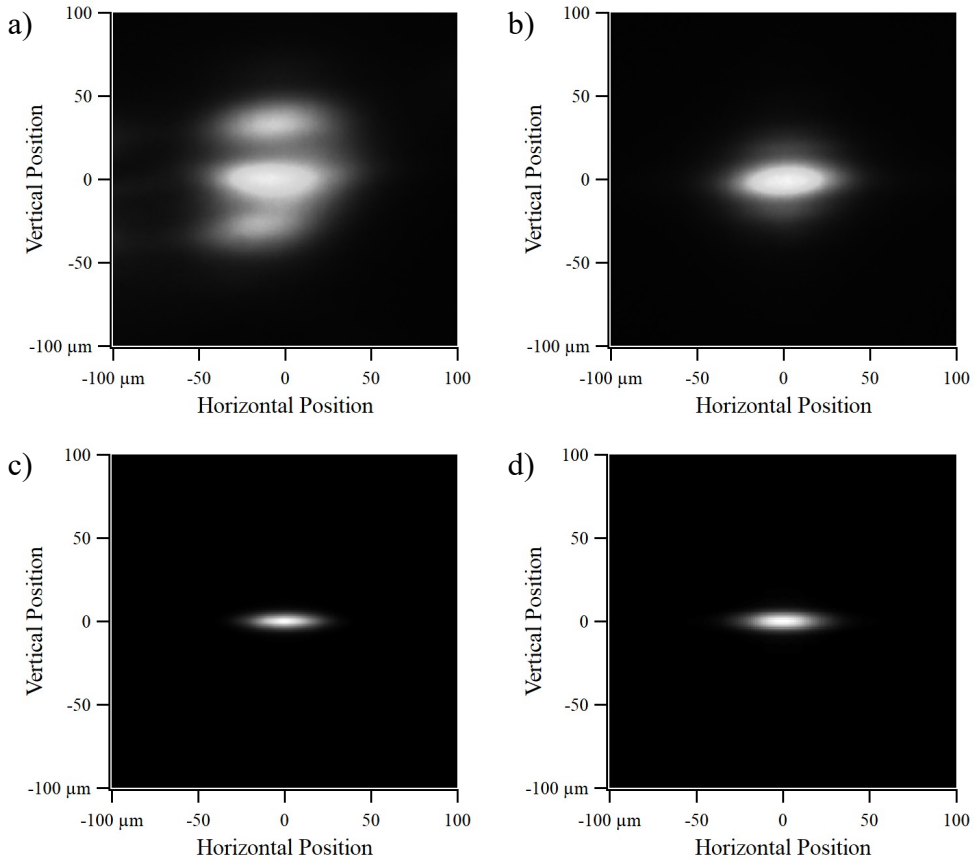

Figure 2. Intensity distributions of ~13.5 keV X-rays focused with 2D diamond CRL at different sizes of rectangular aperture in front of the CRL: a) measurements at 400 x 400 µm^2 aperture size; b) measurements at 100 µm (h) x 200 µm (v) aperture size; c) calculations assuming error-free CRL surfaces at 400 x 400 µm^2 aperture size; d) calculations assuming error-free CRL surfaces at 100 µm (h) x 200 µm (v) aperture size.

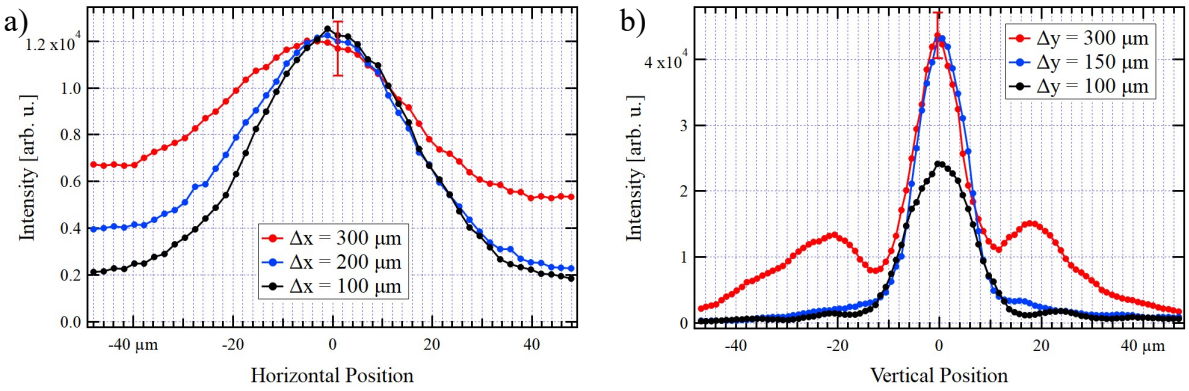

Figure 3. Horizontal (a) and vertical (b) intensity profiles of 13.54 keV X-rays focused with 2D diamond CRL, measured with fluorescent knife-edge at different sizes of the rectangular aperture in front of the CRL (see legends in the graphs).

Intensity profiles of the 13.54 keV UR focused by the diamond CRL at different horizontal and vertical sizes of the aperture before the CRL, measured with the fluorescent knife-edge detectors, are presented in figure 3. One can see aberrations both in the horizontal and in the vertical intensity profiles at 300 µm aperture sizes (manifesting in larger distribution sizes and side lobes in the intensity profiles), that are vanishing with the reduction of the aperture dimensions down to 100 - 200 µm both in the horizontal and vertical direction.

2.3 Comparing measurement results to simulations assuming perfect CRL

To assess the quality of focusing of hard X-rays by the 2D diamond CRL, we compared the measured intensity profiles in the focused X-ray spot at relatively small aperture sizes with the corresponding profiles calculated in the assumption of perfect paraboloid of rotation surface shape of the CRL. Figure 4 shows the measured and calculated horizontal (a, c) and vertical (b, d) intensity profiles, normalized by their corresponding peak values. The constant background that can be seen in figure 3 (a) was removed from the horizontal intensity profiles shown in figure 4 (a, c). The intensity profiles depicted in graphs of figure 4 (a, b) were obtained for the 200 x 200 μm^2 aperture size. Both the horizontal (a) and vertical (b) measured intensity profiles noticeably deviate from the corresponding calculated profiles: the size of the horizontal (vertical) measured profile is ~20% (~60%) larger than the size of the calculated one. The measured and calculated intensity profiles are in much better agreement for smaller aperture sizes, see figure 4 (c, d): for the horizontal aperture of 100 μm (see figure 4 (c)), and for the vertical aperture of 150 μm (see figure 4 (d)) the measured and calculated intensity profiles differ in size by only ~8% in both the horizontal and vertical plane.

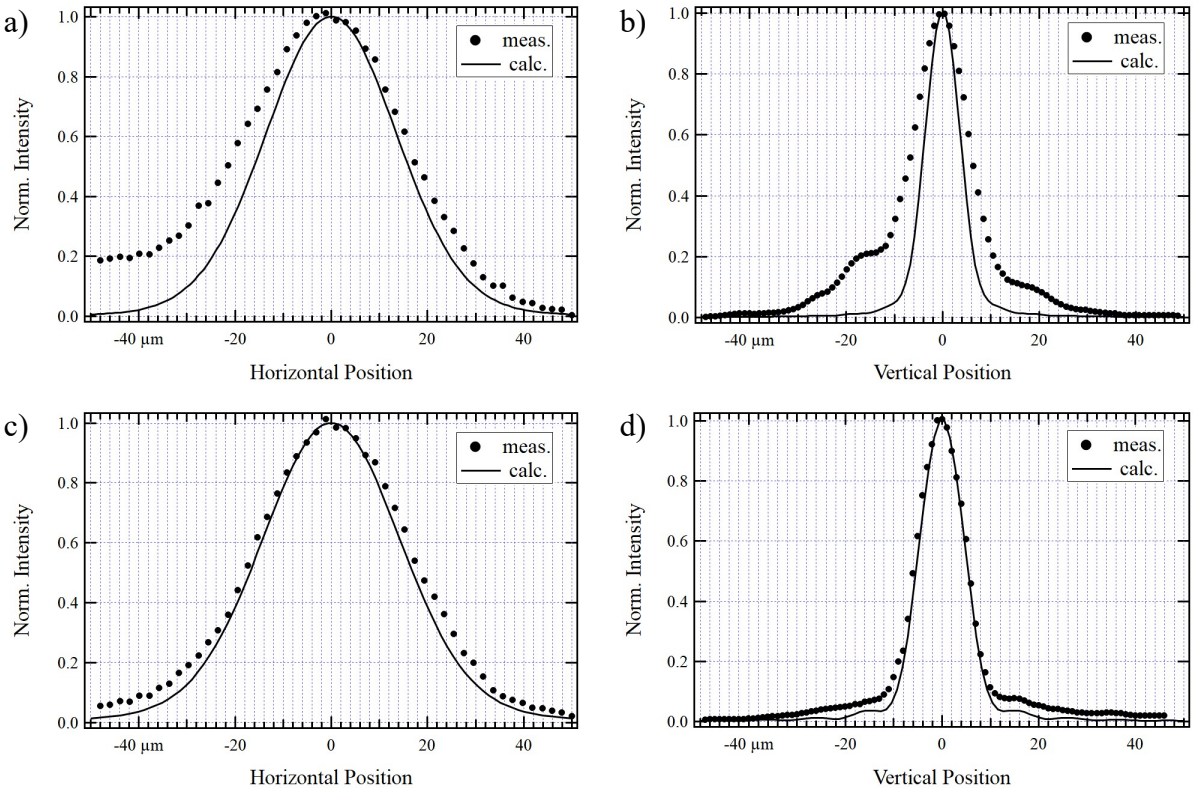

Figure 4. Horizontal (a, c) and vertical (b, d) intensity profiles of ~13.5 keV X-rays focused with 2D diamond CRL measured with fluorescent knife-edge at different sizes of the rectangular aperture in front of the CRL, compared to simulations made at the assumption of error-free paraboloidal surface shape of the CRL: a) horizontal profiles for 200 μm horizontal aperture; b) vertical profiles for 200 μm vertical aperture; c) horizontal profiles for 100 μm horizontal aperture; d) vertical profiles for 150 μm vertical aperture.

We note that the size of the calculated vertical intensity profile is larger at 150 μm aperture than at 200 μm (10.8 μm vs. 8.54 μm) because in the vertical plane, due to small vertical electron beam size, the intensity distribution of UR focused by aberration-free lens is dominated by the diffraction on the aperture installed before the lens. The size of the measured vertical intensity profile, on the other hand, decreased from 13.5 μm to 11.6 μm at the reduction of the vertical aperture from 200 μm to 150 μm. Nevertheless, at further reduction of the vertical aperture to 100 μm, the size of the measured intensity profile increased, to ~15.3 μm (see figure 3 (b)), which is within 10% agreement with calculations. Such a dependence of the focused radiation spot size on aperture size is typical for the focusing by an imperfect lens or mirror, with its imperfections impacting the focused spot stronger at larger apertures.

2.4 Simulating X-ray focusing by imperfect CRL

More simulations were performed to verify if the 2D diamond CRL surface deviation from the perfect paraboloid of rotation, estimated from optical metrology measurements, could explain the measured intensity distributions of the focused X-rays of undulator radiation. The optical metrology data for two surfaces of the 2D diamond CRL used in the tests described in this paper are illustrated in figure 5. Image plots shown in figures 5 (a, b) and 5 (c, d) correspond to surfaces on the "front" and "back" sides on the CRL, with the images (a, c) representing the total measured surface heights as functions of transverse coordinates, and images (b, d) illustrating deviation of the surfaces from paraboloids of rotation.

The results of partially-coherent calculations performed for imperfect CRL, simulated based on the metrology data (see figure 5 (a, c)), with a help of special library developed in SRW [24], are presented in figure 6, where the upper row of graphs (a - c) correspond to 400 x 400 μm^2 size of the aperture before the CRL, and the lower row (d - f) to 150 x 150 μm^2 aperture size. The simulation results shown in figure 6 are in qualitative agreement with the measurement results presented in figures 2 (a, b) and 3. At the large, 400 x 400 μm^2, aperture size, the calculated intensity distribution has side lobes, similarly to the measured one (see figures 2 (a) and 3 (b)), which disappear at the smaller, 150 x 150 μm^2, aperture size, with the latter results being close to the calculations for the error-free CRL surface shape (compare figure 6 (f) to 4 (d)). Some deviations of the calculated intensity distributions for the imperfect CRL from the measurements can be attributed to possible errors in the optical metrology data or its interpretation. Better agreement between the measurements and calculations with imperfect CRL could possibly be reached by adjusting the CRL surface error data to fit the measurement results by the forward simulations, or by applying a phase retrieval algorithm (that should however be valid in the partially-coherent illumination conditions taking place in the measurements under discussion).

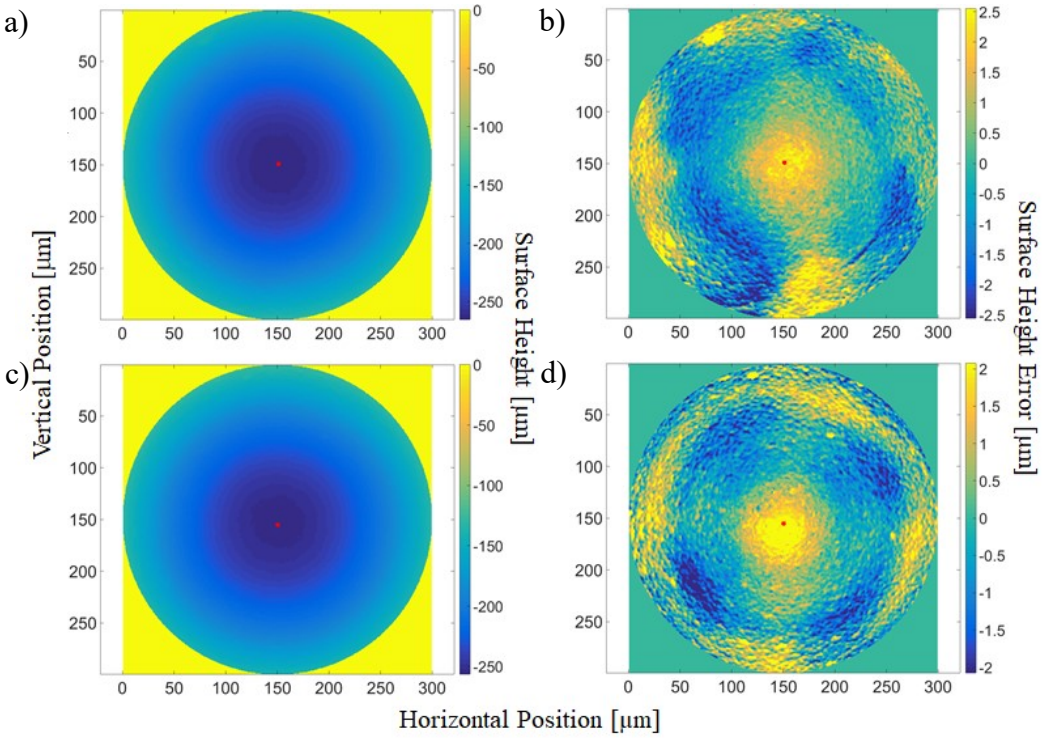

Figure 5. Surface height of the 2D diamond refractive lens from optical metrology measurements: total surface heights on the "front" (a) and "back" (c) sides of the lens, and deviations of these surface heights from the paraboloid of rotation on the "front" (b) and "back" (d) sides.

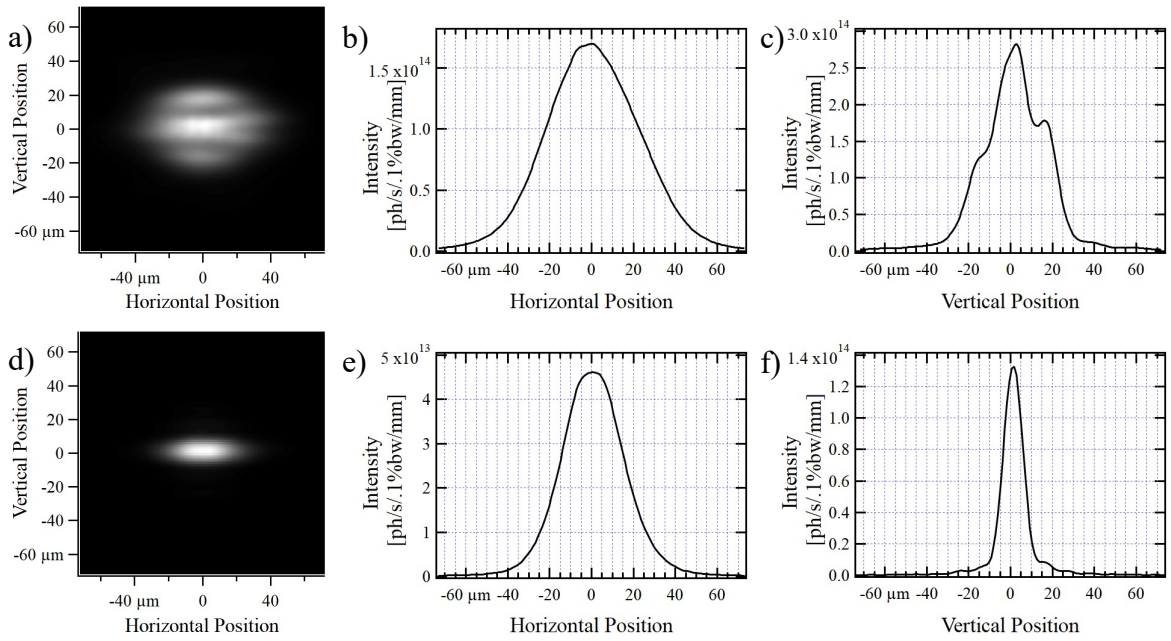

Figure 6. Calculated intensity distributions of ~13.5 keV X-rays of UR focused with imperfect 2D diamond CRL, based on optical metrology data illustrated in figure 5, for 400 x 400 µm^2 (a - c) and 150 x 150 µm^2 size (d - f) aperture before the CRL, including 2D intensity distributions (a, d) and the horizontal (d, e) and vertical (c, f) intensity profiles.

3. MESUREMENTS OF SMALL-ANGLE X-RAY SCATTERING

Besides testing the quality of X-ray focusing by first-generation 2D diamond CRL [17], we have performed measurements of SAXS from it at the same CHX beamline of NSLS-II, that is specialized in coherent X-ray scattering experiments. The SAXS measurements were done in the geometry similar to the one shown in figure 1, with an EIGER 4M detector (having 75 µm square pixel size and 2070 x 2167 numbers of pixels in the horizontal and vertical directions), at 9.65 keV photon energy. The aperture before the CRL was set to 200 x 200 µm^2 size at these measurements. For comparison, we have also performed, in the same experimental conditions, SAXS measurements from 2D Be CRL that had nearly the same focal length at ~13 keV. This "equivalent" Be CRL had 50 µm radius at the tip of parabola, whereas this value of the diamond CRL was 100 µm (note that the refractive index decrement of Be is factor of ~2 smaller than that of diamond at ~13 keV), so the optical path that X-rays made in the body of Be CRL was larger than their path in the body of diamond CRL.

The SAXS measurement results for the diamond and Be CRLs are presented in figure 7: the 2D intensity distributions of scattered X-rays generated by the EIGER detector (with white areas corresponding to missing or damaged pixels, areas obscured by "beam stop", and dominated by slit diffraction) are shown in figure 7 (a, b) as image plots, and the SAXS curves, obtained by circular azimuthal averaging of these 2D intensity distributions, are plotted in figure 7 (c) vs the Q parameter, $Q \approx 2\pi\ \theta_s/\lambda$, where θ_s is angle from the optical axis and λ is the radiation wavelength. As one can readily see from figure 7, the scattering from the Be CRL is considerably, by more than one order of magnitude, higher than the scattering from the diamond CRL, over the whole range of Q-values / angles.

It should be noted that while in the case of Be CRL the X-ray scattering takes place mainly in the CRL volume, in the case of diamond CRL, the scattering is likely to be produced by the CRL surface imperfections. This is supported by the results of other tests, in which the scattering from non-polished diamond CRLs was observed to be considerably higher than from the polished one, that was tested and described in this paper. At the same time, as supported by previous tests of X-ray focusing by Be CRL, its surfaces are likely to be of higher quality than those of the diamond CRL.

The low X-ray scattering produced by diamond CRLs is a very attractive feature, that may allow to extend the range of applications of the CRL optics to areas / experiments that are very sensitive to the background scattering (e.g. those targeting coherent-diffractive-imaging reconstruction of weakly-scattering samples), where Be lenses are not currently used, or are not considered as optics of best choice.

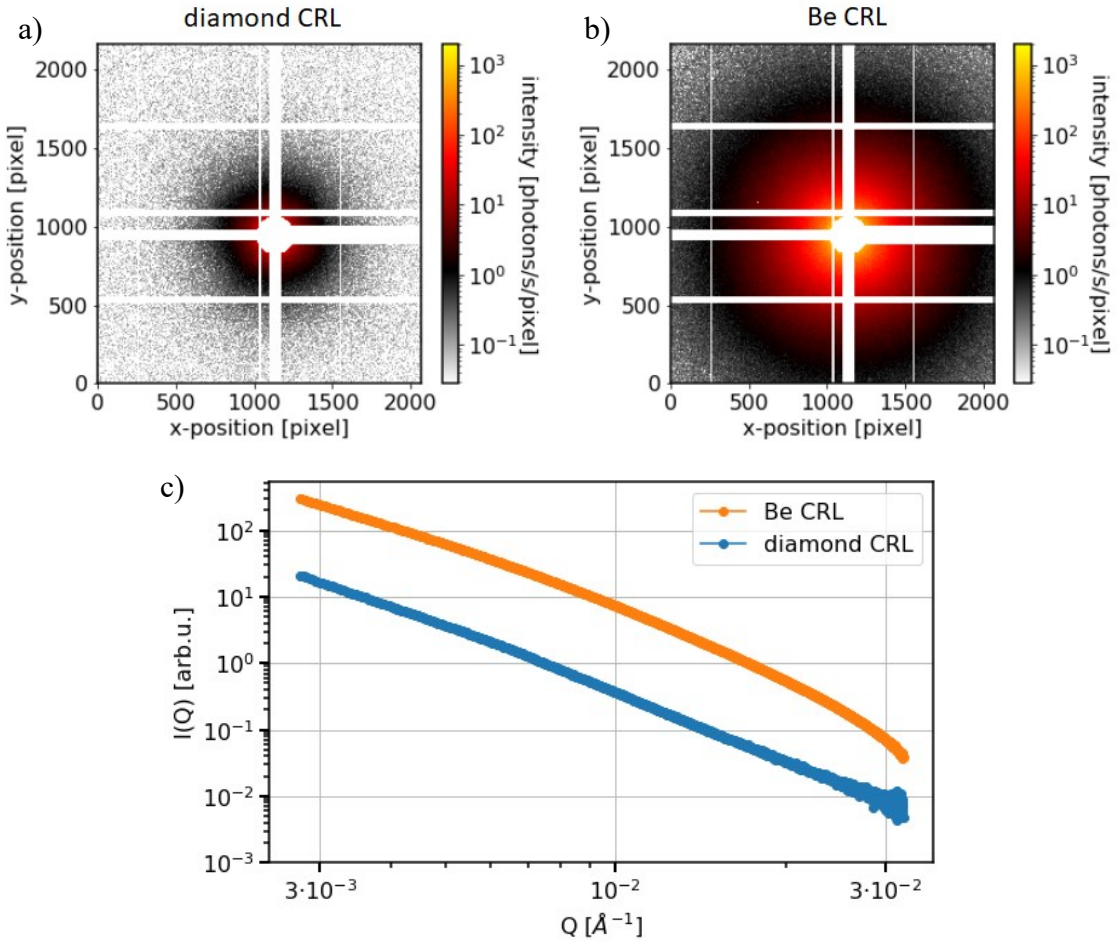

Figure 7. Measured intensity distributions of 9.65 keV UR scattered by diamond and Be CRLs that were used for the focusing tests: 2D intensity distributions generated by EIGER detector located at ~16 m distance from the lenses, for the diamond (a) and Be (b) CRL, and the corresponding azimuthally averaged SAXS curves (c). The scattering measurements were done at the CHX beamline, in the same geometry that was used for the measurements of the X-ray focusing with the CRL, at 200 x 200 μm^2 aperture before the CRL.

4. CONCLUSIONS

Our tests of hard X-ray focusing by first-generation 2D diamond parabolic CRL [17] with geometrical circular aperture diameter of ~400 μm and ~100 μm surface radius at the tip of parabola, performed at the CHX beamline of NSLS-II, demonstrated that this X-ray optical element performs reasonable-quality focusing of the ~13.5 keV undulator radiation beam in low-demagnification geometry, if used with additional aperture of 100 - 200 μm horizontal and vertical size. In particular, for 150 μm and lower vertical aperture size, the focusing performance approaches the diffraction limit, as confirmed by partially-coherent simulations with SRW code. However, when used with a larger aperture, or without any additional aperture, these parabolic CRL produces considerable aberrations in the focused X-ray spot. Further improvement of the surface quality by polishing or other techniques will likely to improve the focusing performance of this type of CRL. A remarkable feature of the diamond CRL was also demonstrated to be its very low small-angle X-ray scattering, which is by more than one order of magnitude lower than the scattering produced by high-quality Be CRL with the same focal length. We believe that the obtained results are very encouraging, and hope that the remarkable progress that was made over the last years in the area of manufacturing of diamond CRLs will continue, and their applications at modern light source facilities will become standard for high-brightness and high-coherence hard X-ray beamlines, for great benefits of science and technology.

ACKNOWLEDGMENTS

The work was supported by DOE SBIR grant DE-SC0013129, DOE BES Field Work Proposal PS-017, and DOE contract DE-SC0012704.

REFERENCES

[1] Snigirev, A., Kohn, V., Snigireva, I., and Lengeler, B., "A compound refractive lens for focusing high-energy X-rays", Nature 384(6604), 49-51 (1996).
[2] Kirz, J. and Attwood, D., "Zone Plates" in X-Ray Data Booklet, Center for X-Ray Optics and Advanced Light Source, Lawrence Berkeley National Laboratory, University of California, Berkeley, CA, pp. 4-27 – 4-31 (2009).
[3] Yan, H., Conley, R., Bouet, N. and Yong S Chu, Y. S., "Hard x-ray nanofocusing by multilayer Laue lenses", J. Phys. D: Appl. Phys. 47, 263001 (2014).
[4] Bajt, S. et al., "X-ray focusing with efficient high-NA multilayer Laue lenses", Light: Science & Applications 7, 17162 (2018).
[5] Chubar, O., Fluerasu, A., Chu, Y.S., Berman, L., Wiegart, L., Lee, W.-K., Baltser, J., "Experimental characterization of X-ray transverse coherence in the presence of beam transport optics", J. Phys.: Conf. Ser. 425, 052028 (2013).
[6] Tavares, P. F. et al., "Commissioning and first-year operational results of the MAX IV 3 GeV ring", J. Synchrotron Rad. 25, 1291-1316 (2018).
[7] Biasci, J. C. et al., "A Low-Emittance Lattice for the ESRF", Synchrotron Radiation News 27 (6), 8 - 12 (2014).
[8] McNeil, B., "First light from hard X-ray laser", Nature Photonics 3, 375–377(2009).
[9] Decking, W. et al., "A MHz-repetition-rate hard X-ray free-electron laser driven by a superconducting linear accelerator", Nature Photonics 14, 391-397 (2020).
[10] Serebrennikov, D., Clementyev, E., Semenov, A. and Snigirev, A., "Optical performance of materials for X-ray refractive optics in the energy range 8-100 keV", J. Synchrotron Rad. 23, 1315-1322 (2016).
[11] Lengeler, B., Schroer, C., Tummler, J., Benner, B., Richwin, M., Snigirev, A., Snigireva, I., and Drakopoulos, M., "Imaging by parabolic refractive lenses in the hard X-ray range", J. Synchrotron Rad. 6, 1153-1167 (1999).
[12] Lengeler, B., Schroer, C., Kuhlmann, M., Benner, B., Gunzler T. F., Kurapova, O., Zontone, F., Snigirev, A., and Snigireva, I., "Refractive x-ray lenses", J. Phys. D: Appl. Phys. 38 A218-A222 (2005).
[13] Chumakov, A., private commun.
[14] Roth, T., Helfen, L., Hallmann, J., Samoylova, L., Kwaśniewski, P., Lengeler, B., Madsen, A., "X-ray laminography and SAXS on beryllium grades and lenses and wavefront propagation through imperfect compound refractive lenses", Proc. SPIE 9207, 920702-1 (2014).
[15] Lyatun, I., Ershov, P., Snigireva, I., and Snigirev, A., "Impact of beryllium microstructure on the imaging and optical properties of X-ray refractive lenses", J. Synchrotron Rad. 27, 44-50 (2020).
[16] Terentyev, S. et al., "Parabolic single-crystal diamond lenses for coherent X-ray imaging", Appl. Phys. Lett. 107, 111108 (2015).
[17] Antipov, S., Baryshev, S. V., Butler, J. E., Antipova, O., Liu, Z., and Stoupin, S., "Single-crystal diamond refractive lens for focusing X-rays in two dimensions", J. Synchrotron Rad. 23, 1 (2016).
[18] Antipov, S. P., Assoufid, L., Grizolli, W. C., Qian, J., Shi, X., "Femtosecond Laser Ablation for Manufacturing of X-ray Lenses and Phase Corrector Plates", Proc. IPAC-2018, 4057-4058, THPMF011 (2018).
[19] Wiegart, L., Rakitin, M., Fluerasu, A., Chubar, O., "X-ray optical simulations supporting advanced commissioning of the Coherent Hard X-ray beamline at NSLS-II", Proc. SPIE 10388, 103880N (2017).
[20] Smaluk, V., Li, Y., Hidaka, Y., Tanabe, T., Chubar, O., Wiegart, L., Blednykh, A., Bacha, B., and Shaftan, T., "Effect of undulators on magnet lattice and emittance", Phys. Rev. Accel. Beams 22, 124001 (2019).
[21] Chubar, O., Elleaume, P., Kuznetsov, S., Snigirev, A., "Physical optics computer code optimized for synchrotron radiation", Proc. SPIE 4769, 145 (2002).
[22] https://github.com/ochubar/SRW
[23] Rakitin, M.S., Moeller, P., Nagler, R., Nash, B., Bruhwiler, D.L., Smalyuk, D., Zhernenkov, M., and Chubar, O., "Sirepo: an open-source cloud-based software interface for X-ray source and optics simulations", J. Synchrotron Rad. 25, 1877-1892 (2018).
[24] Celestre, R., Chubar, O., Roth, T., Sanchez del Rio, M., Barrett, R., "Recent developments in X-ray lenses modelling with SRW", Proc. SPIE 11493, 11493-17 (2020).